

Introduction

- High mass gamma-ray binaries (HMGBs) consist of a massive O or Be type star and a compact object (either NS or BH).
- LS 2883/PSR B1259-63 is one of the best studied HMGBs
- Fast-spinning, massive ($M \sim 30 M_{\odot}$, $L = 6 \times 10^4 L_{\odot}$) star with a strong wind.
- The wind is dense and slow in the equatorial disk, tenuous and fast outside disk.
- Pulsar B1259-63: Spin period = 48 ms, $\dot{E}_{\text{dot}} = 8 \times 10^{35}$ erg/s, Spin-down age = 330 kyr, should emit pulsar wind
- Orbit: 3.4 yr orbital period, 0.87 eccentricity, Orbital inclination $\sim 154^\circ$, pulsar passes through the disk twice each orbit
- Distance = 2.6 kpc

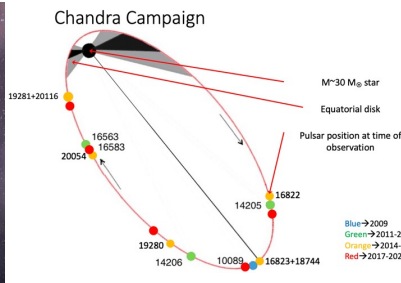
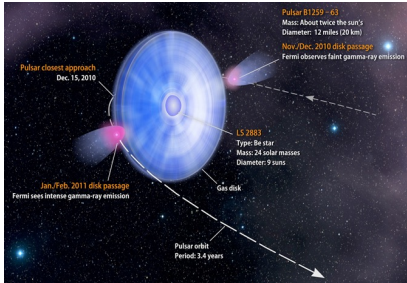


Figure 1 Left: Cartoon of the LS 5883/PSR B1259-63 system. Note the inclination of the decretion disk with respect to the pulsars orbit (credit Francis Reddy NASA/GSFC). Right: Schematic of the LS 5883/PSR B1259-63 system showing the orbital phase of the pulsar in different epochs when our Chandra observations were taken (different colored points). The black circle shows the companion star, while the shaded black and grey regions show the projection of the decretion disk. The orbit is roughly aligned with how the system is viewed on the sky.

2011-2014

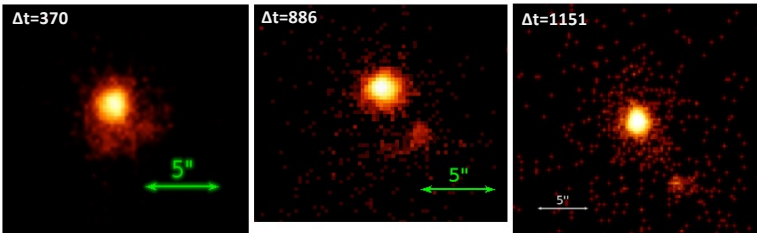


Figure 2 Chandra ACIS images of the B1259 binary in the 2011-2014 binary cycle. The point source is the binary and is not resolved by Chandra. Extended X-ray emission (nicknamed the "clump" can be seen around the binary. The number in the upper left-hand corner is the time since the last periastron passage. Figure adopted and modified from Pavlov et al. (2015).

2014-2017

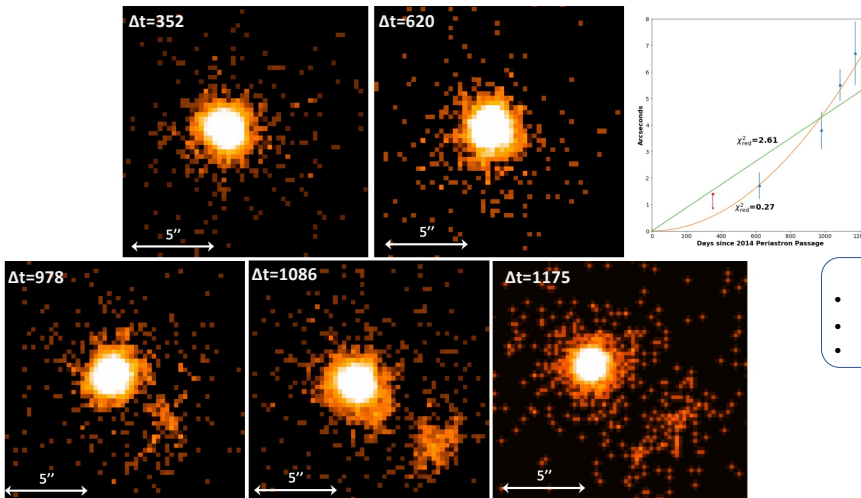


Figure 3 Same as Figure 2, but for the 2014-2017 binary cycle. Note that the clump changes morphology and even brightens in the 5th panel. The figure in the upper-right shows the measured distance of the clump from the binary as a function of time. If we assume the clump was launched near periastron passage, a model including accelerated motion works better than just a constant projected velocity model. Figure adopted and modified from Hare et al. (2019).

Clump motion and characteristics

- Clumps launched in 2 of the 3 observed cycles
 - Photon index of 1.4
- Characteristic size of the "clump" $\sim 3'' \sim 10^{17}$ cm
- $L_X \sim 5 \times 10^{31}$ erg/s of about 5% of the binary luminosity
 - Shows no signs of deceleration!
 - Projected velocities of 10%-15% c.

2017-2021

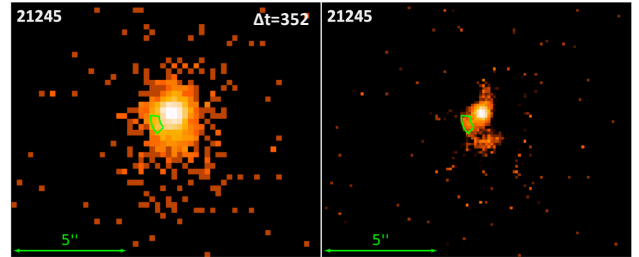


Figure 4 Left: Only Chandra ACIS observation from the 2014-2017 binary cycle to show hints of extended emission. Right: Deconvolved Chandra image, the green region shows the Chandra mirror asymmetry. Evidence of a clump being launched can be seen. However, the clump was not detected in later observations. Figure adopted from Hare et al. (2023).

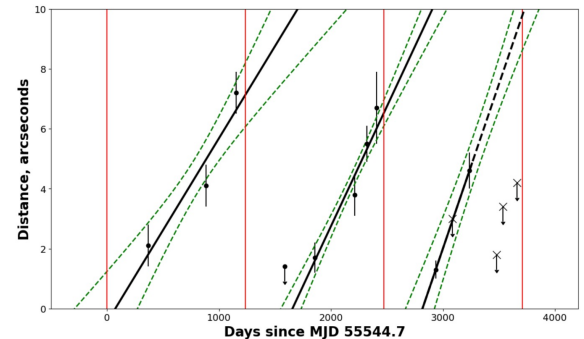


Figure 5 Separation of the clump from the binary as a function of time. The crosses with downward arrows represent upper-limits. The red lines show the times of periastron passages. The fitted lines show the clump's anticipated trajectory overtime, assuming a constant projected velocity. We find projected velocities between 10%-15% c.

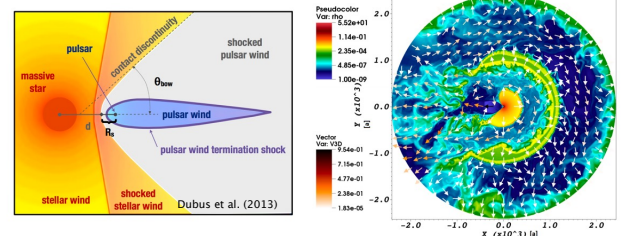
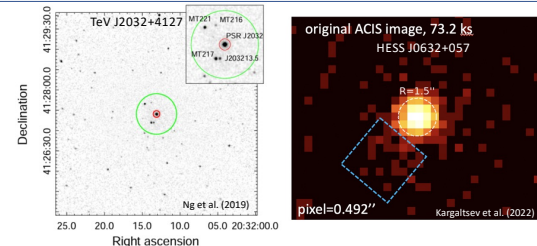


Figure 6 Left: Stellar wind's momentum flux ratio dominating pulsar wind, confines pulsar wind to a channel. Right: Simulation of B1259. Different colors correspond to different density. Colored arrows show velocity vector in units of c. Pulsar wind confined to apastron direction, can interact and accelerate material along the apastron direction. Figure adopted from Barkov and Bosch-Ramon (2016).

Open questions

- What drives the clumps appearance versus non-appearance?
- Are the clumps related to the GeV flares in any way?
- Why are clumps not observed in other HMGBs?



References and Acknowledgements

- Pavlov, G. G., et al. (2011), ApJ, 730, 2
- Pavlov, G. G., et al. (2015) ApJ, 806, 192
- Hare, J., et al. (2019), ApJ, 882, 74
- Hare, J., et al. (2023), arXiv:2309.12156
- Dubus, G. 2013, A&P, 21, 64
- Barkov, M. V. & Bosch-Ramon, V. 2016, MNRAS, 456, L64
- Ng, C.-Y., et al. (2019) 2019, ApJ, 880, 147
- Kargaltsev, O., et al. (2022), ApJ, 925, 20

Support for this work was provided by Chandra Awards GO9-20044X and GO1-22037X, and the Chandra ACIS Team contract SV4-74018.

J. H. acknowledges support from NASA under award number 80GSFC21M0002.